A Low-Complexity Correlation-Based Time Skew Estimation Technique for Time-Interleaved SAR ADCs

Armia Salib, Barry Cardiff and Mark F. Flanagan

School of Electrical and Electronic Engineering, University College Dublin, Ireland

Email: armia.salib-farag@ucdconnect.ie, barry.cardiff@ucd.ie, mark.flanagan@ieee.org

***Abstract*—This paper presents a technique to estimate the time skew in time-interleaved ADCs. The proposed method estimates all of the time skew parameters *jointly* based on observations from a bank of correlators. The proposed method works for an arbitrary number of sub-ADCs. For implementation of the correlator bank, we propose the use of Mitchell's logarithmic multiplier and a hardware reuse mechanism, thereby reducing the complexity and power consumption. Also, we explain why blind estimation techniques alone (including the proposed one) are not always sufficient for time skew estimation for certain classes of input signal; for the proposed approach, however, a simple modification to the analogue circuit (suitable for SAR ADCs) is shown to successfully deal with such problems, with only a minor penalty in power and area. The technique is verified by extensive simulations including a spectrally rich input signal in which an MTPR (multi-tone power ratio) improvement from 29dB to 62dB was achieved for a TIADC system having 16 sub-ADCs.**

***Index terms*—TIADC, time skew, estimation, blind calibration.**

I. Introduction

The TIADC architecture offers high conversion rates; however, it is sensitive to the various mismatches among the M sub-ADCs, including offset, gain, time skew and bandwidth mismatches, which occur due to process, voltage and temperature variations.

In this paper, we focus on time skew mismatches. These cause spurious components (spurs) to occur in the output digital signal, limiting the TIADC's performance; thus it is necessary to use a calibration algorithm to compensate their effects. In general, a calibration technique is composed of two processes, *estimation* and *correction*. The focus of this paper is the problem of accurate time skew estimation under the assumption that the correction can be done either by analog delay lines, e.g., [2-4] or by digital interpolation filters, e.g., [5] and [6].

In blind time skew estimation, the output samples from the TIADC are processed to estimate the time skew mismatches, without the need to make any changes to the analogue circuit. Blind time skew estimation algorithms often compute the correlation between the sub-ADCs' outputs in order to estimate the mismatches. This idea was introduced in [6], targeting $M = 2$, while [2-5] exploit a similar idea for larger M. In [2], only the sign of an error term was used to update a specific sub-ADC's delay line by a specific fixed amount causing the algorithm to have slow convergence. In [3] and [4], in which M is required to be a power of 2, the correlation is measured between the outputs of two *non*-consecutive sub-ADCs having nominal time difference βT_s, where β is a power of 2 less than M. However, both [3] and [4] rely on the assumption that the derivative of the input signal's autocorrelation function is negative at all such time lags βT_s. The algorithm proposed in [5] estimates the time skew using a single block of samples; however, extensive computations, including a non-constant matrix inversion, are needed.

In this paper, we introduce an algorithm to jointly estimate all of the time skew mismatches for a TIADC, based on joint processing of the correlation between the outputs of each pair of consecutive sub-ADCs. For the time skew correction, programmable delay lines are used which are adjusted according to the output of this joint correlation processing. Unlike [3] and [4], the proposed method is applicable to a TIADC structure having any number of sub-ADCs (not only a power of two). The proposed method also does not require any assumptions regarding the sign of the derivative of the input signal's autocorrelation function. Finally, the method shows an MTPR improvement from 29dB to 62dB.

II. Proposed Time Skew Estimation Scheme

Fig. 1 shows a block diagram of the proposed time skew calibration method, which targets a TIADC system with an overall aggregated sampling rate f_s. The TIADC system consists of M slow sub-ADCs; each has sampling rate f_s/M but with different starting phase. However, all sub-ADCs' outputs are synchronized to a single clock with frequency f_s/M. Let $x_n^{(m)}$ denote the n^{th} output of the m^{th} sub-ADC ($m = 0,1, \dots M-1$). Assuming the TIADC system suffers only from the problem of time skew, $x_n^{(m)}$ can be written as

$$x_n^{(m)} \triangleq x\big((nM+m)T_s + \tau_m\big), \tag{1}$$

where $x(t)$ is the analog input signal, and $T_s = 1/f_s$. The time skew residue (the result of the circuit's time skew and the delay imposed by the programmable delay line) affecting the m^{th} sub-ADC is denoted by τ_m, and has nominal value 0. We take the 0^{th} sub-ADC as a timing reference, i.e., $\tau_0 = 0$. For ease of notation we define $x_n^{(M)} \triangleq x_{n+1}^{(0)}$, and $\tau_M \triangleq \tau_0 = 0$.

We define the autocorrelation function of $x(t)$ as $R_{xx}(\tau) = \lim_{T\to\infty} \frac{1}{T}\int_0^T x(t)x(t+\tau)\,dt$, and we compute M estimates of $R_{xx}(\tau)$ in the vicinity of $\tau = T_s$, each denoted by c_m, as follows

$$c_m \triangleq \frac{1}{N}\sum_{n=0}^{N-1} x_n^{(m+1)}\, x_n^{(m)} \tag{2}$$

$$\approx R_{xx}(T_s + \tau_{m+1} - \tau_m) \quad \forall\, m \in \{0,..,M-1\}, \tag{3}$$

where N is selected to be a large number, and the above approximation is due to the discrete and finite nature of the

This publication has emanated from research supported by S3group, Dublin, Ireland, and in part by a research grant from Science Foundation Ireland (SFI) and is co-funded under the European Regional Development Fund under Grant Number 13/RC/2077.

summation in (2). It is assumed for this work that the input signal, $x(t)$, is such that the approximation in (3) holds. This is the case for overwhelmingly many input signals; however, as outlined in Section IV, there are some exceptions.

A first-order approximation for (3) is given by

$$c_m \approx R_{xx}(T_s) + \frac{dR_{xx}(T_s)}{d\tau}(\tau_{m+1} - \tau_m), \tag{4}$$

where $\frac{dR_{xx}(T_s)}{d\tau}$ is the autocorrelation function derivative for $x(t)$ at T_s. The differences between adjacent c_m lead to

$$e_m \triangleq c_m - c_{m-1} \qquad \forall\, m \in \{1, .., M-1\} \tag{5}$$

$$\approx -\frac{dR_{xx}(T_s)}{d\tau}(-\tau_{m-1} + 2\tau_m - \tau_{m+1}). \tag{6}$$

Writing these equations in matrix form, we obtain

$$\boldsymbol{e} \approx -\frac{dR_{xx}(T_s)}{d\tau}\boldsymbol{U}\boldsymbol{\tau}, \tag{7}$$

where $\boldsymbol{e} \triangleq (e_m)_{m\geq 1}$ and $\boldsymbol{\tau} \triangleq (\tau_m)_{m\geq 1}$ are $(M-1)\times 1$ vectors, and $\boldsymbol{U}$ is an $(M-1)\times(M-1)$ symmetric Toeplitz matrix having first row filled with zeros except for the first and second entries which are equal to 2 and -1, respectively. Equation (7) can be used to evaluate $\boldsymbol{\tau}$ as follows

$$\boldsymbol{\tau} \approx -\left(\frac{dR_{xx}(T_s)}{d\tau}\right)^{-1}\boldsymbol{U}^{-1}\boldsymbol{e}, \tag{8}$$

where $\boldsymbol{U}^{-1}$ is a constant matrix, $\boldsymbol{e}$ is measured in accordance with equations (2) and (5), and $\frac{dR_{xx}(T_s)}{d\tau}$ is a scalar which can be estimated as will be explained in Subsection III.A below.

This procedure differs from the previous works in that we use *all* of the values e_m to aid in the estimation of *each* τ_m. Note in particular that it was assumed in [3] and [4] that $\frac{dR_{xx}(\beta T_s)}{d\tau}$ is negative for β equal to any power of 2 less than M; while this assumption is usually valid for $\beta = 1$, it often does not hold for $\beta > 1$.

III. Implementation

The target of the blind estimation technique is to adapt the delay line of each sub-ADC in order to compensate the time skew residue which is measured using (8), forming a closed-loop feedback system that is adapted iteratively. In each *calibration iteration*, the following procedure is executed:

1- Using a block of N samples from each of the M sub-ADCs, we calculate $\boldsymbol{e}$ and $\frac{dR_{xx}(T_s)}{d\tau}$.

2- Using (8), the time skew residues for this block are then estimated, and the programmable delay lines are adapted accordingly prior to repeating Step 1 for the next block.

The following subsections highlight important elements in the implementation of these steps.

A. Autocorrelation derivative

For band-limited input signals, [3] and [4] ignores the term $\frac{dR_{xx}(T_s)}{d\tau}$, assuming that this term is always negative. This does not affect the *direction* of adaptation of the subsequent

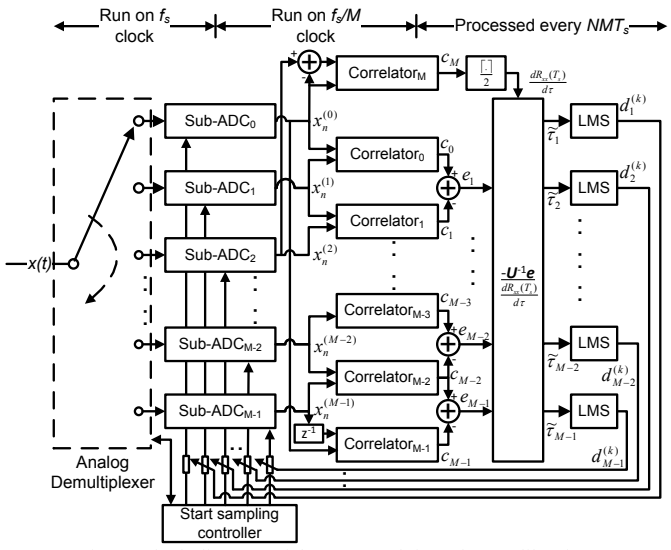

Fig. 1. Block diagram of the proposed time skew calibration.

programmable delay lines; however, it makes the convergence speed dependent on the input signal. To avoid this dependency, our proposed algorithm estimates this term, which can be written as

$$\frac{dR_{xx}(T_s)}{d\tau} = \lim_{T\to\infty}\int_0^T x(t)x'(t+T_s)dt, \tag{9}$$

where $x'(\cdot)$ is the derivative of the analog input signal. We may estimate (9) from the sub-ADCs' output samples via

$$\frac{dR_{xx}(T_s)}{d\tau} \approx \frac{1}{N}\sum_{n=0}^{N-1} x_n^{(0)}\left[\frac{x_n^{(2)} - x_n^{(0)}}{2T_s}\right], \tag{10}$$

where the term in square brackets approximates the first derivative of $x(t)$ at time $t = (nM+1)T_s$. This requires an extra correlator to perform the correlation of $x_n^{(0)}$ and $\left[x_n^{(2)} - x_n^{(0)}\right]$; this is shown in Fig. 1 as $\mathrm{Correlator_M}$.

B. Low-complexity correlator

A correlator consists mainly of a multiplier and an adder running on a clock with frequency f_s/M. To avoid the multiplier complexity and reduce its power, we propose to simplify its hardware implementation at the expense of its accuracy, where the effect of the introduced inaccuracy is relaxed due to averaging. We chose to use Mitchell's logarithmic multiplier architecture [1] where the base-2 logarithms of the two inputs are approximated, summed together, and the result taken to the power of two. This simplifies the multiplier to mainly an adder, two priority encoders and three bit-shifters.

The application of this low-complexity multiplier is particularly useful for our present context, as different correlators share the same inputs, and thus hardware resource sharing can be employed to further reduce both area and power.

C. Adaptation

Using NM samples, the c_m are computed, for $m \in \{0,1,\ldots,M\}$, using a bank of correlators; the first M of these are used to compute $\boldsymbol{e}$ using (5), and c_M is used to estimate $\frac{dR_{xx}(T_s)}{d\tau}$ according to (10).

Then, by substituting the estimates of $\frac{dR_{xx}(T_s)}{d\tau}$ and $\boldsymbol{e}$ into (8), we compute $\tilde{\boldsymbol{\tau}}$, an estimate of the $\boldsymbol{\tau}$. This is then used to adapt each $d_m^{(k)}$, the m^{th} programmable delay line configuration in the k^{th} calibration iteration, with adaptation step size μ according to

$$d_m^{(k)} = d_m^{(k-1)} - \mu\tilde{\tau}_m \;\; \forall m \in \{1,..,M-1\}. \qquad (11)$$

The elements in $\boldsymbol{U}^{-1}$ can be precomputed; note however that each element can be represented up to a scaling factor using exactly $\lceil \log_2 M \rceil$ bits. Also note that, as there is no tight constraints on the adaptation timing, the multiplications required for $\boldsymbol{U}^{-1}\boldsymbol{e}$ can be done sequentially, requiring only one multiplier and an accumulator.

Note that for implementation, all constant scaling factors can be rounded to the nearest power of 2 numbers to reduce the complexity, since a closed loop adaptation mechanism is used.

IV. Limitations of Blind Estimation

The proposed method depends on the validity of the approximation in (3) (note that the same assumption is also required in the works [2-6]). This approximation, while valid for a wide range of input signals, can be inaccurate in the case of at least two 'pathological' input signal types, leading to incorrect time skew estimation:

1- An input signal containing components at frequencies $k\frac{f_s}{2M}$, for $k \in \{0,..,M-1\}$. A solution to this, as suggested in [2] and [6], is to use a notch filter to remove these components.

2- An input signal containing multiple frequency components, some of which appear like the spurs of others. The blind estimator cannot distinguish between the spurs generated by the time skew and the input signal itself. Note that simple filtering will not be able to resolve this issue.

The co-existence of the second pathological type with other non-problematic frequency components has a dramatic impact on blind estimation convergence. To assess this, we measured the SFDR after calibration for an 11-bit $M = 2$ TIADC using an input signal consisting of 10 sinusoids with randomly selected frequencies. The output spectrum is shown in Fig. 2a; the measured SFDR is 68dB. However, the SFDR becomes limited to 21dB when two sinusoids with frequencies $(111/1024)f_s$ and $(1/2 - 111/1024)f_s$ are added as shown in Fig. 2b. This demonstrates that the existence of such problematic frequency components leads to incorrect blind estimation convergence even in the presence of other non-problematic components.

V. Sampling Sequence Intervention

The existence of the limitations reported in Section IV decreases the blind estimation robustness, and thus a method is required to overcome these limitations with only a minor penalty in area and power. Thus, we introduce a small change to the analogue circuitry, consisting of a minor intervention in the TIADC's sampling sequence, whereby the analog de-multiplexer and the 'start sampling controller' blocks shown in Fig. 1 both skip a sub-ADC every N samples. Note that in general, the application of this modification requires that a complete conversion shall be finished within $(M-1)T_s$, thus

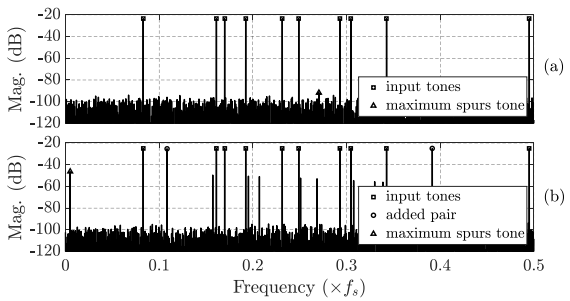

Fig. 2. Spectrum of the ADC output after blind calibration using an input consisting of 10 randomly selected sinusoids: (a) without problematic components, (b) with problematic components.

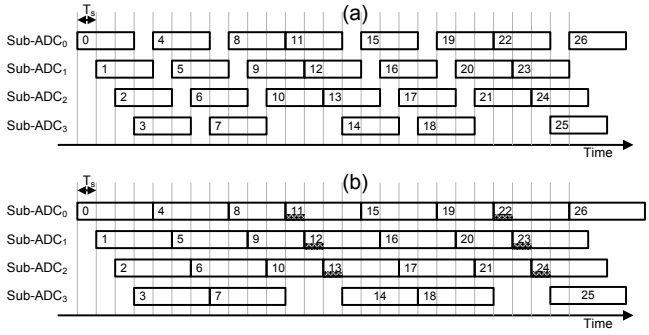

Fig. 3. The timing diagram is illustrated for a TIADC with $M = 4$, and $N = 11$, where a conversion is finished within: (a) $(M-1)T_s$, (b) MT_s.

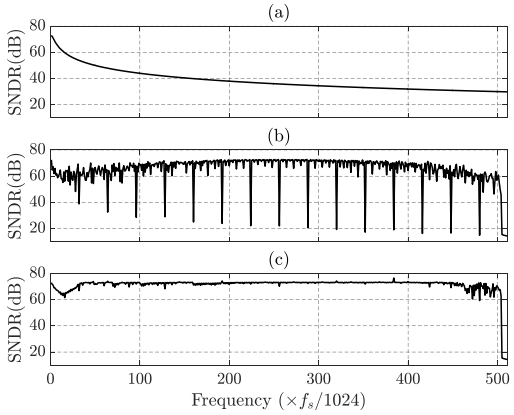

Fig. 4. Measured SNDR (a) without calibration, (b) with calibration and normal sampling sequence, (c) with calibration and sequence intervention.

tightening the constraints on the analogue circuit. Fig. 3a shows the corresponding timing diagram for $M = 4$ and $N = 11$.

However, in this work we target a successive approximation register (SAR) sub-ADC architecture, where a complete conversion cycle is divided into smaller parts to resolve each output bit; this permits forcing an *early termination* for the conversion cycle without losing all of the sampled bits. Hence, we can design the sub-ADC to perform a complete conversion within MT_s, and an early termination for T_s is forced only when a sequence intervention occurs. Fig. 3b shows the proposed timing diagram for $M = 4$ and $N = 11$; in contrast to Fig. 3a, a complete conversion is usually allowed to take MT_s. The forced early terminated periods are partially shaded. For large M, if T_s is less than the time taken to resolve the least significant bit (LSB), then only $M-1$ samples out of every N will each lose one LSB.

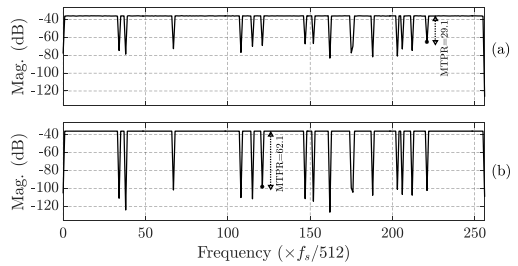

Fig. 5. PSD for the ADC's output (a) without calibration, (b) with calibration.

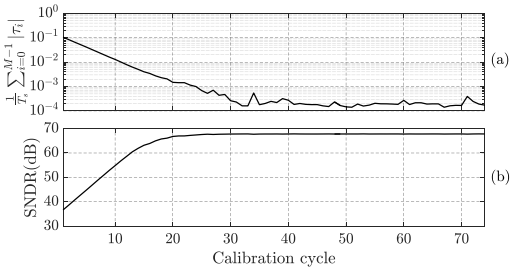

Fig. 6. The convergence of (a) the normalized sum of the absolute values of the time skew residues, (b) the SNDR.

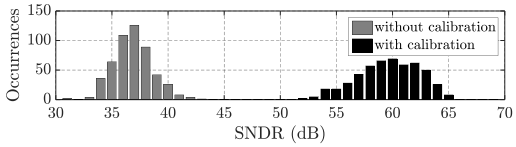

Fig. 7. Measured SNDR histogram using band-limited input signal.

In practice, N is selected to be a large number in order to minimize the sequence intervention rate. Since sequence intervention occurs rarely, and indeed only during the time skew estimation process, the performance loss associated with the early termination events is negligible. We also note that to avoid the impact of the sequence intervention on the calculation of c_m in (2), the output samples around the intervention event are not considered in the outputs of all the correlators.

VI. Simulation Results

The presented estimation technique is verified using three tests targeting a 12-bit TIADC with $M = 16$. Early-terminated samples have a resolution of 11-bit. The sub-ADCs suffer from time skew with standard deviation $0.01T_s$, and ideal programmable delay lines are used to apply the correction. Here we have chosen $N = 8191$.

In the first test, a sinusoidal input was used, with frequency sweeping from 0 to $f_s/2$ with step size $f_s/1024$. The reported results are obtained after 75 calibration iterations. Fig. 4 shows the measured SNDR with and without calibration. Since the sequence intervention is not used in Fig. 4b, the measured SNDR suffers from dramatic degradation at the frequencies reported in Section IV. However, as can be seen in Fig. 4c, the SNDR is almost immune to these problems when the sequence intervention technique is used. Both approaches exhibit a sudden breakdown with input frequency greater than $504f_s/1024$. However, for wideband signals, these high-frequency components do not affect the estimation mechanism as verified in the next test.

The second test verifies the time skew estimation performance with an OFDM-like input consisting of sinusoids with frequencies $if_s/512, \forall i \in \{1,..,255\}$, random phases, and equal amplitudes except for 16 randomly selected frequency components which have zero amplitude. Since M is even, the blind detector can converge to incorrect values without the use of sequence intervention, because almost every frequency component appears like the spur of another. Using the proposed estimation technique, the power spectral density of the ADC's output without and with calibration is shown in Fig. 5; after 75 calibration iterations the SNDR is improved from 34dB to 67dB, and the MTPR is improved from 29dB to 62dB. Also, Fig. 6 shows the convergence of the normalized sum of the absolute values of the time skew residues, as well as the evolution of the SNDR during the calibration process.

The third test uses a signal consisting of independent and identically distributed (i.i.d.) uniform time domain samples, which is then low-pass filtered with bandwidth $0.85f_s/2$; the resulting band-limited signal is typical of many real-world applications. This test was repeated 510 times. For each test, the SNDR was measured after 600 calibration iterations. Fig. 7 shows the histogram for the measured SNDR; on average, the SNDR is improved from 36.8dB to 59.6dB.

VII. Conclusion

In this paper, a time skew estimation technique is presented that can be used for a TIADC system with any number of sub-ADCs. A low-complexity correlators based on Mitchell's multiplier are used to minimize power consumption and area. Although the presented technique itself can be considered as a blind method, we explained why this technique is not alone sufficient for accurate blind time skew estimation in all cases of input signal type, and we showed how to introduce a minor sampling sequence intervention mechanism, particularly suitable for SAR ADC architecture, in order to overcome this limitation. The resulting increased robustness of the estimator comes at the cost of a minor reduction in the TIADC's output precision during the (rarely occurring) sequence intervention events. A tradeoff may be made by choosing appropriately the value of N. Finally, we verified the proposed estimation technique using three tests with different input signal characteristics.

References

[1] J. Mitchell, "Computer multiplication and division using binary logarithms," *IRE Transactions on Electronic Computers*, vol. EC-11, no. 4, pp. 512-517, Aug. 1962.

[2] Q. Lei, Y. Zheng, D. Zhu, and L. Siek, "A statistic based time skew calibration method for time-interleaved ADCs," *IEEE International Symposium on Circuits and Systems*, pp. 2373–2376, June 2014.

[3] H. Wei, P. Zhang, B. Sahoo, and B. Razavi, "An 8-Bit 4-GS/s 120-mW CMOS ADC," *IEEE Journal of Solid-State Circuits*, vol. 49, no. 8, pp. 1751–1751, Aug. 2014.

[4] L. Wang, Q. Wang, and A. Carusone, "Time interleaved C-2C SAR ADC with background timing skew calibration in 65nm CMOS," *European Solid State Circuits Conference*, pp. 207–210, Sept. 2014.

[5] N. Le Dortz, J. Blanc, T. Simon, S. Verhaeren, E. Rouat, and P. Urard, "A 1.62GS/s time-interleaved SAR ADC with digital background mismatch calibration achieving interleaving spurs below 70dBFS," *IEEE International Solid-State Circuits Conference*, pp. 386–388, Feb. 2014.

[6] S. Jamal, D. Fu, N. Chang, P. Hurst and S. Lewis, "A 10-b 120-Msample/s time-interleaved analog-to-digital converter with digital background calibration," *IEEE Journal of Solid-State Circuits*, vol. 37, no. 12, pp. 1618–1627, Dec. 2002.